RESEARCH ARTICLE

Integrative single-cell transcriptome analysis provides new insights into post-COVID-19 pulmonary fibrosis and potential therapeutic targets

Yumin Kim[1] | Yeongmin Kim[1] | Hyobin Julianne Lim[2] | Dae-Kyum Kim[2] | Ji-Hwan Park[3,4] | Chang-Myung Oh[1] (iD)

[1]Department of Biomedical Science and Engineering, Gwangju Institute of Science and Technology, Gwangju, Republic of Korea

[2]Department of Cancer Genetics and Genomics, Roswell Park Comprehensive Cancer Center, Buffalo, New York, USA

[3]Korea Bioinformation Center, Korea Research Institute of Bioscience & Biotechnology, Daejeon, Republic of Korea

[4]Department of Bioscience, University of Science and Technology (UST), Daejeon, Republic of Korea

Correspondence
Ji-Hwan Park, Korea Bioinformation Center, Korea Research Institute of Bioscience & Biotechnology, Daejeon 34141, Republic of Korea.
Email: jhpark706@kribb.re.kr

Chang-Myung Oh, Department of Biomedical Science and Engineering, Gwangju Institute of Science and Technology, Gwangju 61005, Republic of Korea.
Email: cmoh@gist.ac.kr

Abstract

The global COVID-19 pandemic caused by the severe acute respiratory syndrome coronavirus 2 virus has resulted in a significant number of patients experiencing persistent symptoms, including post-COVID pulmonary fibrosis (PCPF). This study aimed to identify novel therapeutic targets for PCPF using single-cell RNA-sequencing data from lung tissues of COVID-19 patients, idiopathic pulmonary fibrosis (IPF) patients, and a rat transforming growth factor beta-1-induced fibrosis model treated with antifibrotic drugs. Patients with COVID-19 had lower alveolar macrophage counts than healthy controls, whereas patients with COVID-19 and IPF presented with elevated monocyte-derived macrophage counts. A comparative transcriptome analysis showed that macrophages play a crucial role in IPF and COVID-19 development and progression, and fibrosis- and inflammation-associated genes were upregulated in both conditions. Functional enrichment analysis revealed the upregulation of inflammation and proteolysis and the downregulation of ribosome biogenesis. Cholesterol efflux and glycolysis were augmented in both macrophage types. The study suggests that antifibrotic drugs may reverse critical lung fibrosis mediators in COVID-19. The results help clarify the molecular mechanisms underlying pulmonary fibrosis in patients with severe COVID-19 and IPF and highlight the potential efficacy of antifibrotic drugs in COVID-19 therapy. Collectively, all these findings may have significant implications for the development of new treatment strategies for PCPF.

KEYWORDS
antifibrotic agent, idiopathic pulmonary fibrosis, post-COVID-19 pulmonary fibrosis, singe-cell transcriptomics

1 | INTRODUCTION

The novel coronavirus strain designated as severe acute respiratory syndrome coronavirus 2 (SARS-CoV-2) is the causative agent of coronavirus disease 2019 (COVID-19). It first emerged in Wuhan, China, in 2019 and since then, has rapidly spread worldwide.[1] In March 2020, the World Health Organization (WHO) declared COVID-19 a pandemic. As of December 2022, over 659 million confirmed cases of COVID-19 and more than 6.7 million deaths had been reported globally.[2] Most patients presented with mild symptoms and recovered within 1–2 weeks.[3] However, certain individuals exhibited persistent symptoms that lasted for several weeks or months. This condition was designated as "long COVID."[4]

COVID-19 pneumonia may induce fibrotic lung damage known as post-COVID pulmonary fibrosis (PCPF), which is a frequent complication in patients with long COVID-19.[5] Between 45% and 54% of all hospitalized COVID-19 survivors experience lung fibrosis.[6] Even after 1 year, one-third of all patients with moderate COVID-19 present with fibrotic changes and severe impairment of the diffusing capacity for carbon monoxide in the lungs (DLCO).[7] There have also been reports of cases of pulmonary fibrosis following asymptomatic COVID-19 infection.[8] In general, patients with pulmonary fibrosis have a poor quality of life and require additional medical care.[9,10] The high prevalence of PCPF has become a severe problem worldwide.[11] Nevertheless, its underlying mechanism is unclear and a cure is yet to be developed.[7]

Idiopathic pulmonary fibrosis (IPF) is a chronic, debilitating lung disease characterized by abnormal fibrotic tissue accumulation in the lungs. It results in progressive lung function impairment and eventually causes respiratory failure.[12] The precise molecular mechanisms underlying IPF development are elusive. However, several antifibrotic drugs, such as nintedanib and pirfenidone, have been approved for IPF treatment.[13] These drugs inhibit the fibrotic process and have lowered mortality in patients with IPF.[12] Furthermore, they have improved lung function in patients suffering from other forms of fibrotic lung disease.[14]

IPF and PCPF share similar clinicopathological features, such as reduced DLCO, disrupted alveolar-capillary barriers, renin-angiotensin-aldosterone system imbalance, increased oxidative stress, and chronic inflammation. Hence, they both may respond to similar therapeutic strategies.[5,15] In the present study, we profiled single-cell gene expression in the lung tissues of COVID-19 and IPF patients. Comparative single-cell transcriptome analyses revealed altered abundance and activity of individual cell types, prioritizing certain key cell types, cellular processes, signaling pathways, and genes may be common to both IPF and PCPF pathophysiology. We also compared gene expression profiles in the lungs of a rat transforming growth factor beta-1 (TGF-β1)-induced pulmonary fibrosis model treated with antifibrotic agents. This integrated approach elucidated the pathogenesis of the fibrotic changes associated with COVID-19 infection and facilitated the identification of novel therapeutic modalities against PCPF.

2 | METHODS

2.1 | Single-cell RNA seq data analysis

Publicly available raw data (GSE149878, GSE145926, and GSE158127) were downloaded and then Cell Ranger[1] (10× genomics; v. 6.1.1) was used for mapping to the GRCh38 human reference genome and then loaded using the Seurat[2] package (v. 4.1.1). Given processed data was available (GSE122960), raw_feature_bc_matrix.h5 file was loaded also using Seurat package. Because we used processed data from GSE122960, the versions of the reference genome in GSE149878 and GSE122960 did not match. Before merging two independent data sets (GSE149878 and GSE122960) reference genome matching was performed by filtering out mismatched gene. The corrected count matrices were combined through the Seurat[2] package and quality control was conducted. In brief, empty droplets were excluded using the EmptyDrops function in the DropletUtils[3] (v. 1.16.0) package in R at false discovery rate (FDR) < 0.01. Detailed information on the methods used in this study can be found in the Supporting Information. Sample characteristics are summarized in Table S1.

3 | RESULTS

3.1 | Similar cell abundance alterations in the lung tissues of both COVID-19 and IPF patients reveal potential regulatory cell types in fibrosis

We performed an integrative data analysis using multiple publicly available data sets to determine the key cell types, cellular processes, signaling pathways, and genes of human pulmonary fibrosis (Figure 1A). These sources included single-cell RNA-Seq data from patients diagnosed with severe COVID-19 (GSE149878), those presenting with severe IPF, and control subjects (GSE122960). We used the fluorescence-activated cell sorting-sorted scRNA-Seq data set obtained from COVID-19 patients and control subjects (GSE158127) and the scRNA-seq data set of bronchoalveolar lavage fluid from severe and mild COVID-19 patients and control subjects (GSE145926) to validate our analysis. Additionally, we incorporated bulk RNA-seq data derived from a rat TGF-β1-induced fibrosis model with or without administration of antifibrotic drugs, such as nintedanib, sorafenib, and pirfenidone (GSE120679). We integrated two independent data sets with batch correction (GSE122960 and GSE149878) to disclose pathophysiological similarities between IPF and PCPF and performed gene expression profiling of 94 005 cells without two samples due to highly biased cell type fractions (Figure S1a,b). Uniform manifold approximation and projection results corroborated the similarities between the gene expression profiles of COVID-19 and IPF relative to those of the Control (Figure S1c). We performed cell clustering and cell type annotation and identified 21 cell types and their distinct marker genes (Figure 1B,C). To prioritize potential regulatory cell types in fibrosis, we examined the differences in lung cell composition among the Control, COVID-19, and IPF groups (Figure 1D, Table S2). The COVID-19 group had higher proportions of mature and immature neutrophils
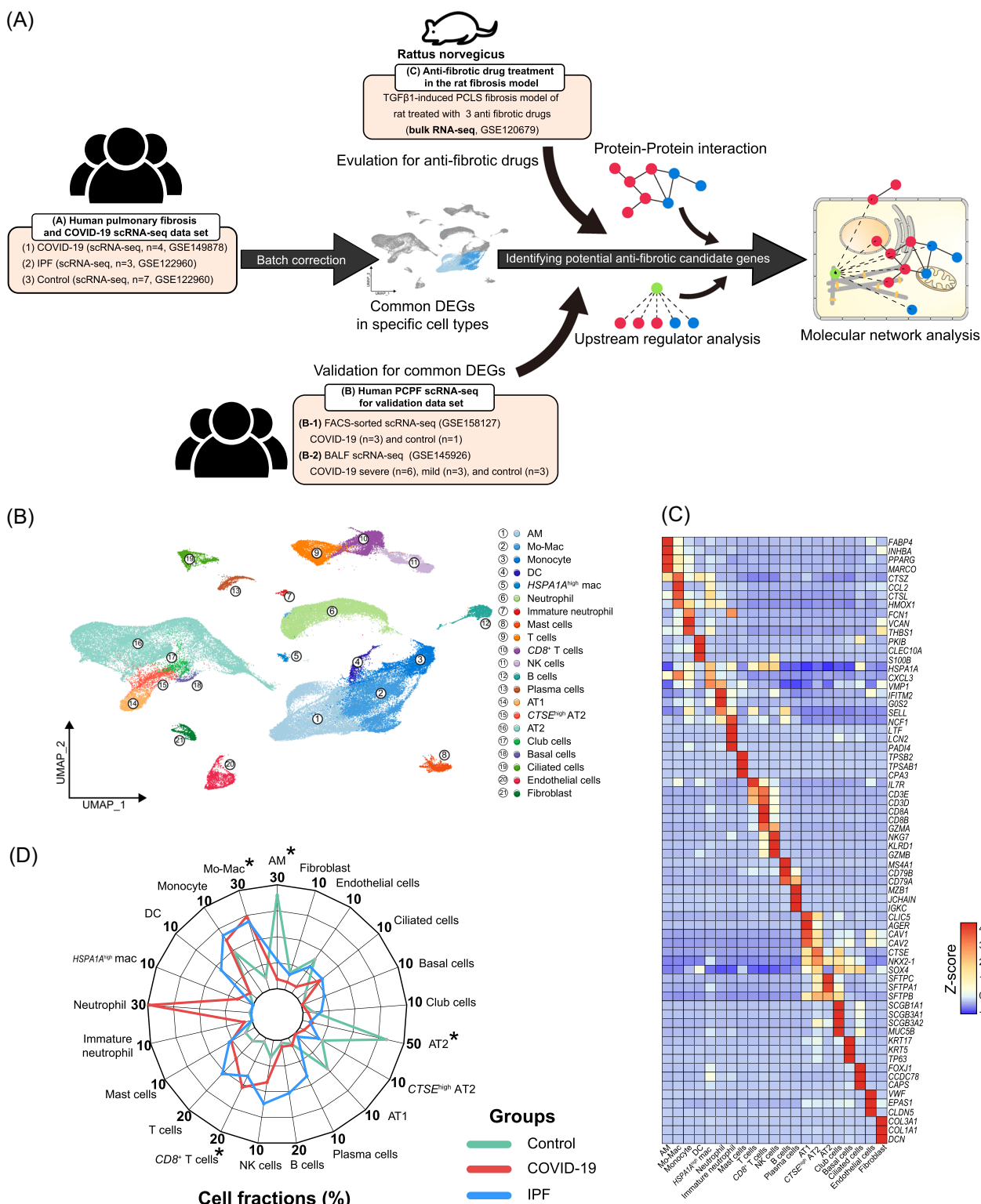
FIGURE 1 Similar changes in cell abundance in lung tissues of COVID-19 and, idiopathic pulmonary fibrosis (IPF) patients reveal potential regulatory cell types in fibrosis. (A) Workflow of comparative analysis. Two independent single-cell RNA-seq data were integrated (data set A). Data sets B-1 and B-2 were used for validation of common differentially expressed genes (DEGs) and data set C was used to evaluate antifibrotic drugs for common DEGs. Molecular network analysis includes information on protein–protein interactions, analysis of upstream regulators, validation, and whether gene expression is reversed by antifibrotic drugs. (B) UMAP of cells obtained from two independent studies (GSE149878 and GSE122960). (C) Heatmap showing expression of marker genes associated with different cell types. (D) Cell-type fractions in patients and donors were averaged for each group. Each group is assigned a different color. The number under the cell types in the panel indicated the maximum range of cell type fractions starting at zero. Significant differences in the COVID-19 versus control and IPF versus control comparisons are denoted by *($p < 0.05$; two-way analysis of variance). UMAP, uniform manifold approximation and projection.

than the Control and IPF groups. Both the COVID-19 and IPF groups exhibited significant ($p < 0.05$) decreases in alveolar macrophages (AMs) and alveolar type II cells (AT2) relative to those in the Control. Conversely, there were significantly ($p < 0.05$) higher monocyte-derived macrophages (Mo-Macs) and $CD8^+$ T cell fractions in the COVID-19 and IPF groups than in the Control. These findings suggested the four cell-types (AMs, AT2 cells, Mo-Macs, and $CD8^+$ T cells) as the potential regulatory cell types, contributing to the pathophysiological similarities between PCPF- and IPF-associated fibrosis.

3.2 | Common alterations in the activity of regulatory cell types suggest key cellular processes and genes in both IPF- and PCPF-associated fibrosis

To investigate alterations in the cellular activity of the four potential regulatory cell types, we identified the differentially expressed genes (DEGs) for each cell type by comparing the gene expression profiles of COVID-19 and IPF against those of the Control group. For COVID-19, we identified 524, 268, 455, and 450 DEGs in AMs, Mo-Macs, AT2 cells, and $CD8^+$ T cells, respectively. For IPF, we identified 190, 267, 291, and 62 DEGs in AMs, Mo-Macs, AT2 cells, and $CD8^+$ T cells, respectively (Figure S2a). We examined the overlap of DEGs between COVID-19 and IPF to prioritize the key cell types showing similar changes in gene expression in both conditions. Only AMs and Mo-Macs significantly ($p < 0.00001$) shared DEGs (Figure S2a). Hence, these cell types may contribute to the pathophysiology of both IPF and PCPF in terms of both cell abundances and activities to clarify molecular characteristics of 94 and 129 DEGs in AMs and Mo-Macs, respectively (Figure 2A and Table S3). Genes related to fibrosis and inflammation, such as secreted phosphoprotein 1 (SPP1), S100 calcium-binding protein A8 (S100A8), and S100A9,[16,17] were commonly upregulated while those encoding inhibin subunit beta A (INHBA) were downregulated in the two types of macrophages of COVID-19 and IPF compared to levels in the Control.

To investigate the cellular processes and signaling pathways regulated by AMs and Mo-Macs in both COVID-19 and IPF, we performed functional enrichment analysis of gene ontology biological process and kyoto encyclopedia of genes and genomes (KEGG) pathways using the upregulated and downregulated DEGs common to each cell type with various other cell types and disease conditions (Figure 2B). Several KEGG pathways and gene ontology terms were significantly ($p < 0.05$) represented by the upregulated regardless of cell type. These included lysosome biogenesis and function, antigen processing and presentation, proteolysis, mononuclear cell migration, response to wounding, inflammatory response, chemotaxis, and cell adhesion. The ribosome biogenesis and function were significantly downregulated in both COVID-19 and IPF macrophages (Figure 2B). The DEGs related to lipid metabolism (cholesterol metabolism and lipid transport) were commonly upregulated in AMs, whereas those associated with carbohydrate metabolism (carbohydrate metabolic process, pyruvate metabolic process, and glycolytic process) were commonly upregulated in the Mo-Macs of both COVID-19 and IPF.

The foregoing findings were validated using two independent single-cell RNA-seq data sets from other COVID-19 patients with fibrosis (GSE158127 and GSE145926, Figure S2b–e). DEGs analysis was performed for COVID-19 (B-1, and B-2) with control of each data set (Table S3). To confirm that DEGs from IPF versus Control were also detected in other data sets, COVID-19 versus Control was compared in data set B-1. The dot plot shows that 77 and 56 genes were common in AM and Mo-Mac, respectively, across two data sets (Figure S2f). Additionally, to identify how common DEGs were similar among independent single-cell RNA-seq data sets, DEG ID similarity was determined using Sørensen–Dice coefficient. Among the COVID-19 data sets, some common DEGs were conserved, although the mild COVID-19 data set exhibited a little overlap for common DEGs (Figure S2g). Additionally, functional enrichment analysis of both macrophages in each data set revealed similar enrichment across data sets, but weak enrichment in common DEGs (Figure S2h). We then endeavored to elucidate the associations among various biological terms. To this end, we used a process network analysis based on the Sørensen–Dice coefficient to analyze the similarity of the genes belonging to each term. We identified 21 clusters and classified them into immune, metabolism, oxidative stress, ribosome, and other groups (Figure 2C). Figure 2D shows how significantly each term in the process network analysis was up-, downregulated, or both. Terms significantly enriched in AMs and Mo-Macs were colored (Figure S2i). AMs were weakly enriched in clusters related to ribosome, actin cytoskeleton organization, and response to reactive oxygen species but strongly enriched in cytokine production pathways. Mo-Macs were weakly enriched in cytokine production and apoptotic process. Cholesterol metabolism was enriched in AMs, while glycolysis was enriched in Mo-Macs (Figures 2D and S2i).

3.3 | Transcriptomic analysis of the impact of antifibrotic drugs on a rat TGF-β1-induced pulmonary fibrosis model

We investigated how antifibrotic drugs affect gene expression in the lungs of rats with TGF-β1-induced pulmonary fibrosis. To this end, data set C was employed (GSE120679). We explored the potential of these drugs as therapeutic interventions against PCPF. Nintedanib,[18,19] pirfenidone,[20] and sorafenib[21] were administered to a rat model of TGF-β1-induced pulmonary fibrosis, and a bulk RNA-seq analysis was conducted on the lung tissue samples.[22] We compared the transcriptomic profiles of the lung tissues of untreated rats (Negative control), those with TGF-β1-induced pulmonary fibrosis (Fibrosis group), those with TGF-β1-induced pulmonary fibrosis, and nintedanib treatment (Nintedanib group), those with TGF-β1-induced pulmonary fibrosis and pirfenidone treatment (Pirfenidone group), and those with TGF-β1-induced pulmonary fibrosis and sorafenib treatment (Sorafenib group).

A principal component analysis (PCA) showed that the Nintedanib group presented with a gene expression profile comparable to that of the TGFβ1-induced fibrosis group. Moreover, the Pirfenidone group was distinct from those subjected to the other antifibrotic drugs (Figure S3a). The heatmap in Figure 3A illustrates the DEGs
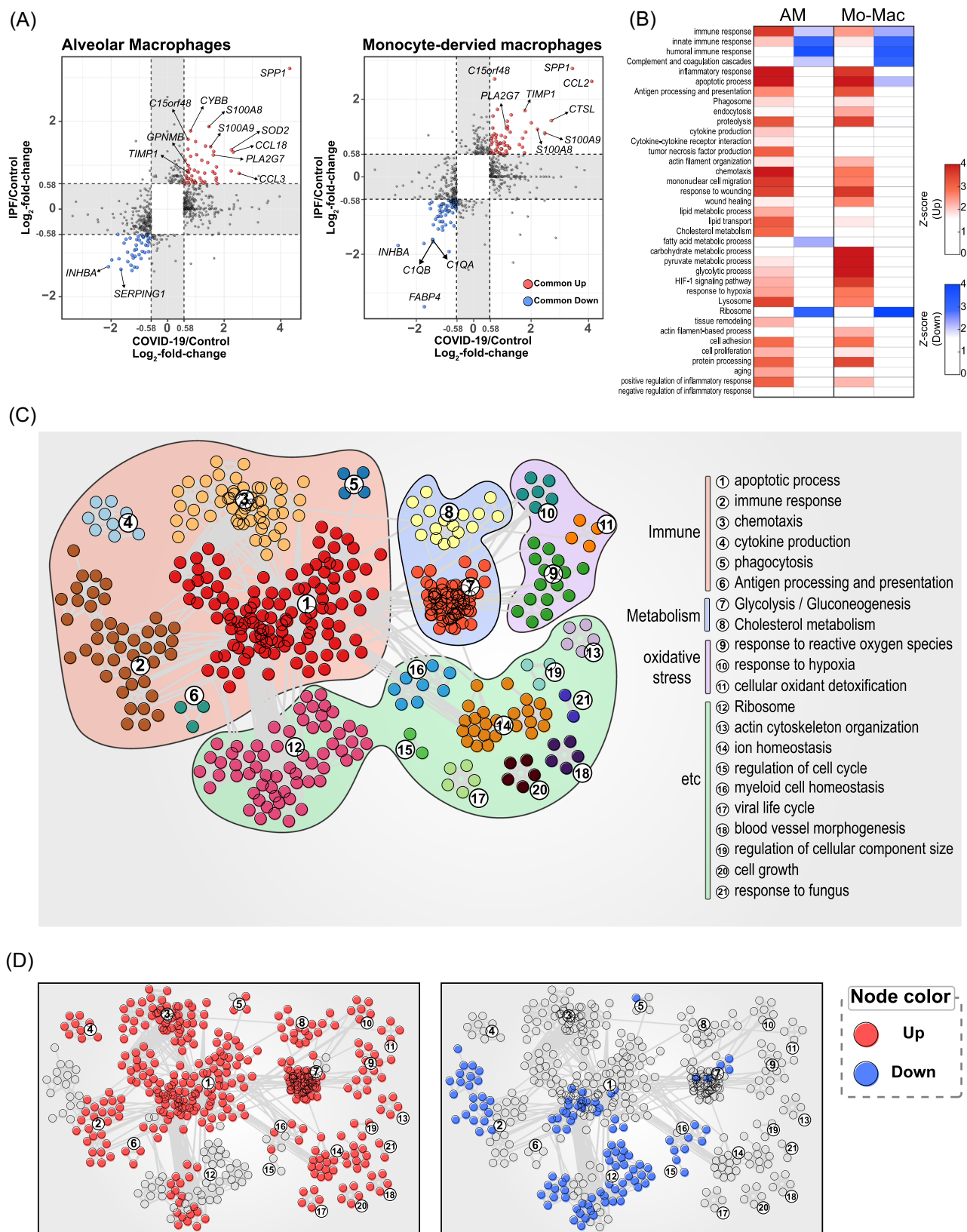
FIGURE 2 (See caption on next page).

between the lung transcriptomes of the Negative control group and those of the fibrosis group. Figure 3B shows that a significant number of genes were altered in response to the antifibrotic drug treatment compared to TGFB1-induced fibrosis samples. Patterns P1, P2, P3, and P4 comprise the genes that were significantly down-, up-, up-, and downregulated, respectively, in the Fibrosis group compared with those in the Negative control group. After antifibrotic drug treatment, the expression of genes in P1 and P2 were upregulated and downregulated, respectively, by at least one antifibrotic drug. Genes in P1 and P2 were defined as "Reversed genes" that switched expression levels after the antifibrotic drug treatments. We then quantified the prevalence of reversed genes in the three antifibrotic drug treatment groups. The Sorafenib group exhibited the highest density of reversed genes (Figure S3b,c and Table S3). The heatmap of gene expression (Figure 3B) illustrates that pirfenidone-induced exclusively dynamic changes in gene expression, whereas sorafenib induced the most changes in gene expression in reversed genes.

Next, we conducted a functional enrichment analysis on each antifibrotic drug. The TGFβ1-induced fibrosis group exhibited reduced immune response, complement coagulation cascades, increased extracellular matrix organization, collagen fibril organization, angiogenesis, and transforming growth factor beta receptor signaling pathway. Among the three antifibrotic drugs, sorafenib most reversed the TGFβ1-induced alteration of biological pathways (Figure S3d). Figure 3C shows that most of the genes reversed by antifibrotic drugs were associated with key molecular pathways involved in the development of pulmonary fibrosis, including inflammation, immune response, and tissue remodeling.[23] Hence, antifibrotic drugs may target the critical pathogenic mechanisms underlying the development of pulmonary fibrosis. We compared the gene expression data with the data set (C) to assess how antifibrotic drugs alter the expression of verified genes identified by the two validation data sets. The expression of a total of 113 validated common DEGs was determined in the antifibrotic drug data set (C), and pirfenidone reversed gene expression the most followed by sorafenib (Figure 3D). Furthermore, we examined whether validated or not at least one validation data set for all cell types and whether those genes were reversed by at least one antifibrotic drug. Sixteen genes satisfied the criteria, of which downregulation of surfactant genes (*SFTPC*, *SFTPD*, and *SFTPB*) in epithelial cells was a common characteristic, and collagen genes (*COL1A1*, *COL3A1*) in fibroblast were highly upregulated (Figure S3e).

3.4 | Integrated analysis of the molecular networks associated with pulmonary fibrosis

We aimed to reveal the vital pathways that must be targeted in PCPF treatment. To this end, we compared the profiles of COVID-19, IPF single-cell RNA, and antifibrotic drug-treated lung transcriptomes with reversed genes (Figure 4). We then integrated these data sets and constructed molecular networks using protein–protein interaction (PPI), upstream regulator analyses, and functional enrichment analysis of common DEGs. The predicted molecular networks in the AMs and Mo-Macs of fibrotic lung tissues are shown in. Lipid metabolism was significantly altered in both types of macrophages during fibrosis. The genes encoding apolipoprotein E[24,25] and *SPP1*[16,17] were upregulated in fibrotic lung tissues. These proteins play important roles in pulmonary inflammation and fibrosis (Figure 4). Phospholipase A2 group VII (*PLA2G7*) was also upregulated, and this enzyme is linked to oxidized low-density lipoprotein. We also identified a key mediator of COVID-19 pathogenesis.[26] Genes controlling antigen processing and chemotaxis were upregulated, whereas those regulating the complement system were downregulated. We also validated these changes in other single-cell RNA-seq data set B-1 (Figure S4a). SARS-CoV-2 may suppress mRNA translation in host cells.[27,28] Our analysis showed downregulation of the genes regulating ribosome function in both macrophage types.

We also detected the upregulation of glycolysis-related genes in Mo-Macs. Glycolysis is a critical feature of M1 macrophages.[29] In the lung, elevated glycolysis under hypoxia may play crucial roles in Mo-Mac survival and lung fibrosis activation. The enolase 1 (*ENO1*) gene was upregulated in both AMs and Mo-Macs in fibrotic lung tissues (Figure 4). *ENO1* expression was upregulated in pulmonary fibrosis.[30,31] Thus, ENO1 is a key enzyme in the metabolic reprogramming of fibrotic lung and a potential therapeutic target for PCPF.

We performed PPI network and upstream regulator analyses to identify the hub genes associated with lung fibrosis. Figures 4 and S4a show the predicted interactions among shared genes related to the key pathways in both COVID-19 and IPF. The URA predicted that *GRN* is the most significant, negative upstream regulator in AMs and also confirmed in COVID-19 validation data sets (Figure S4b,c). Granulin (*GRN*) was identified as the most significant hub gene in both groups and was highly expressed in AMs (Figure S4d). *GRN* controls macrophage polarization.[32] The genes regulating cholesterol

FIGURE 2 Alterations in regulatory cell type activity common to both idiopathic pulmonary fibrosis (IPF) and post-COVID pulmonary fibrosis indicate key cellular processes and genes in both types of fibrosis. (A) Dot plot of $\log_2$-FC of COVID-19 and IPF versus Control showing 94 and 129 common differentially expressed genes (DEGs) in alveolar macrophages (AMs) and monocyte-derived macrophages (Mo-Macs), respectively. Each gene is a DEG in at least one group when comparing COVID-19 versus Control and IPF versus Control. Gray dots represent DEGs found in only one disease group. The log2-FC cutoff is 0.58, and the adjusted p value (p adj. val) is 0.01. (B) Functional enrichment analysis of common DEGs in AMs and Mo-Macs. (C) Process network analysis of GOBP and KEGG pathways that were clarified using the common DEGs in AMs and Mo-Macs. Clusters were grouped based on their functionality. Representative GO or KEGG in each cluster are shown in the right panel along with the cluster number. Each node indicates a GOBP or KEGG pathway. Edge thickness indicates similarity between their DEGs determined with the Sørensen–Dice coefficient. (D) Significant meaningful terms are colored in red and blue, which correspond to upregulated and downregulated nodes, respectively. GO, gene ontology; GOBP, gene ontology biological process; KEGG, kyoto encyclopedia of genes and genomes.
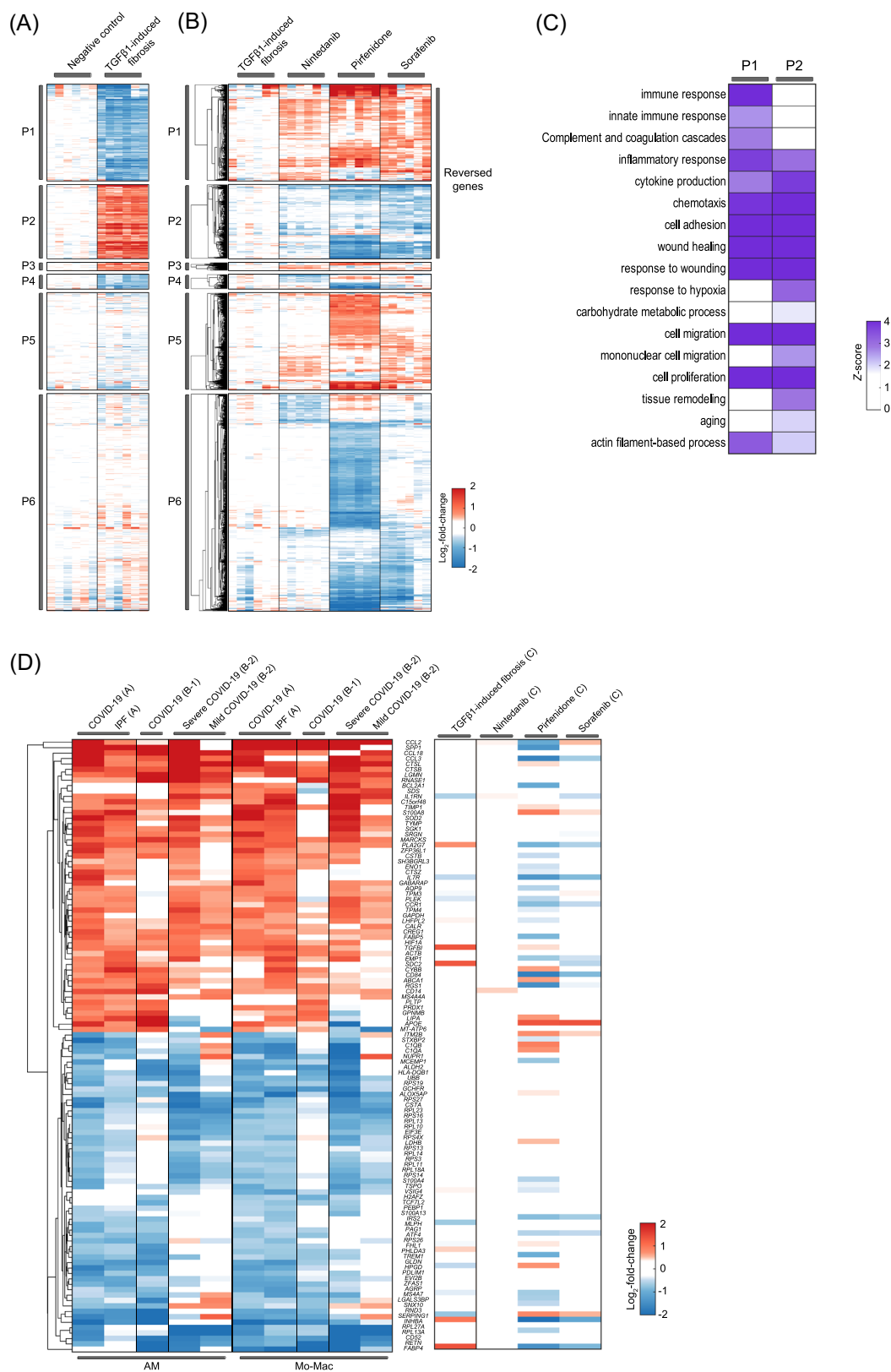
FIGURE 3 (See caption on next page).

efflux, antigen processing, chemotaxis, and complement and coagulation cascades were also important in AMs (Figure 4). In addition, chemotactic cytokines, recognized as a prominent risk factor contributing to the onset of cytokine storm, were found to be upregulated in both macrophages (Figure 4).[33] Inhibitors of these chemotactic cytokines have been proposed as a novel therapeutic target for the treatment of pulmonary fibrosis.[34]

4 | DISCUSSION

We performed a comparative analysis of single RNA-seq data sets of human pulmonary fibrosis obtained from patients with severe COVID-19 and IPF. We identified 21 distinct cell types in the lung and revealed the differences in cellular composition among the COVID-19, IPF, and Control groups. Recent studies showed that chemokine ligand 2 (CCL2) signaling is a key mediator of lung fibrosis[35] and is associated with severe immunopathogenesis in COVID-19.[36,37] Inhibitors of C-C chemokine receptor type 2 (CCR2), the main CCL2 receptor, demonstrated therapeutic potential in both animal and human studies.[38–40]

In both COVID-19 and IPF cohorts, a significant increase in the expression of genes associated with fibrotic pathways was observed. For instance, collagen gene upregulation was observed in fibroblasts in both COVID-19 and IPF patient cohorts (Figure S3e). This finding is consistent with a recent study by Das et al.[41] characterizing the molecular profiles of COVID-19. The authors emphasized the crucial role of collagen genes in the pulmonary pathology resulting from COVID-19. Additionally, they uncovered the activation of IL6-STAT3 and TGF-b-SMAD2/3 signaling pathways in SARS-CoV-2 virus-infected cells. Our results showed that these pathways were reversed after treatment with antifibrotic agents (Figure S3d). Furthermore, the expression level of COL1A1 was highly correlated with the proximity of fibroblasts to infiltrating macrophages or monocytes.[41] These results in spatial levels, support that fibroblast and infiltrated macrophages were key pathology players in PCPFs.

Both the COVID-19 and IPF groups presented with decreases in AMs and increases in Mo-Macs. A pathway analysis showed that the genes related to fibrosis and inflammation were upregulated in both COVID-19 and IPF AMs and Mo-Macs. Genes mediating lipid metabolism were upregulated in COVID-19 and IPF AMs, while those mediating glycolysis were enriched in COVID-19 and IPF Mo-Macs. A process network analysis revealed that the COVID-19 and IPF AMs were weakly enriched in cytoskeleton organization and reactive oxygen species response and strongly enriched in cytokine production, while COVID-19 and IPF Mo-Macs were weakly enriched in both cytokine production and apoptotic process. The molecular signatures common to both COVID-19 and IPF indicate that the antifibrotic drugs administered for IPF treatment have potential therapeutic value against COVID-19 as well. We analyzed the impact of antifibrotic drugs on the transcriptome of a rat model of TGF-β1-induced lung fibrosis. Nintedanib, sorafenib, and pirfenidone effectively reversed the expression of lung fibrosis-related genes, including syndecan-2 (SDC2),[42] PLA2G7,[43] and serpin family G member 1 (SERPING1),[44] common to COVID-19, IPF, and TGF-β1-induced lung fibrosis transcriptomes.

We also observed upregulation of the genes related to cholesterol efflux, including ATP binding cassette subfamily A member 1 (ABCA1), which is a vital transporter enabling cholesterol efflux.[45] ABCA1 prevents lung inflammation and fibrosis by promoting surfactant production.[46] A recent single-cell RNA-seq study disclosed that PLA2G7 is upregulated in macrophages and is linked to fibroblast-to-myofibroblast transition,[43] in addition to being a potential PCPF driver.[47] A drug screening assay showed that the PLA2G7 inhibitor darapladib is a therapeutic candidate for COVID-19.[48] Our findings showed that PLA2G7 was upregulated in the lungs of COVID-19 patients, and its expression was reversed by antifibrotic drugs. This discovery might explain the mechanism underlying the potential benefit of antifibrotic drugs to patients with COVID-19.[49]

We found that glycolysis was upregulated in Mo-Macs. Glycolysis enables inflammatory immune cells to generate metabolic energy rapidly.[29,50] The SARS-CoV-2 virus induces metabolic changes in immune and respiratory endothelial cells.[51] Nevertheless, the results of the present study suggested that antifibrotic drugs did not reverse the expression of genes related to glycolysis, including ENO1. Therefore, antifibrotic drugs alone may not provide optimal COVID-19 treatment. Administration of the glycolysis inhibitor 2-deoxy-D-glucose suppressed SARS-CoV-2 multiplication in vitro and provided clinical benefits to COVID-19 patients in a phase II clinical trial.[52]

It is intriguing and worthy of further discussion that there was a marked increase in genes related to lysosome and proteolysis in both AMs and Mo-Macs (Figure 2B). These findings are consistent with previous reports on the importance of lysosome and proteolysis in coronaviruses. Ghosh et al. recently suggested that lysosomal exocytosis is an important mechanism for coronavirus egress.[53] Meyer et al. have suggested the critical role of proteolytic cleavage of viral and cellular proteins in SARS-CoV-2 replication.[54,55] This finding implies a potential

---

FIGURE 3 Transcriptomic analysis of the impact of antifibrotic drugs on a rat TGFβ1-induced pulmonary fibrosis model. (A, B) Heatmap showing gene expression induced by antifibrotic drugs in the negative control and rat TGFβ1-induced fibrosis groups (A) and in rat TGFβ1-induced fibrosis and antifibrotic drug-treated groups (B). Gene expression was divided into six patterns denoted by P1–P6. Genes in P1 and P2 correspond to downregulated-to-upregulated (negative control vs. fibrosis group and fibrosis vs. antifibrotic drug groups) and upregulated-to-downregulated, respectively, and are defined as reversed genes. Genes in P3 and P4 correspond to upregulated-to-upregulated and downregulated-to-downregulated, respectively. Antifibrotic drug-mediated upregulated and downregulated genes are denoted P5 and P6, respectively. Hierarchical clustering was applied to each group. (C) Functional enrichment analysis of the reversed gene sets corresponding to P1 and P2. Each row in the heatmap corresponds to Figure 2B. (D) Relative gene expression heatmap for 113 validated common DEGs in alveolar macrophages or monocyte-derived macrophages (left panel) and corresponding relative gene expression heatmap (right panel) in rat antifibrotic drug treatment data sets. Each color represents comparison groups previously denoted. TGF-β1, transforming growth factor beta-1.
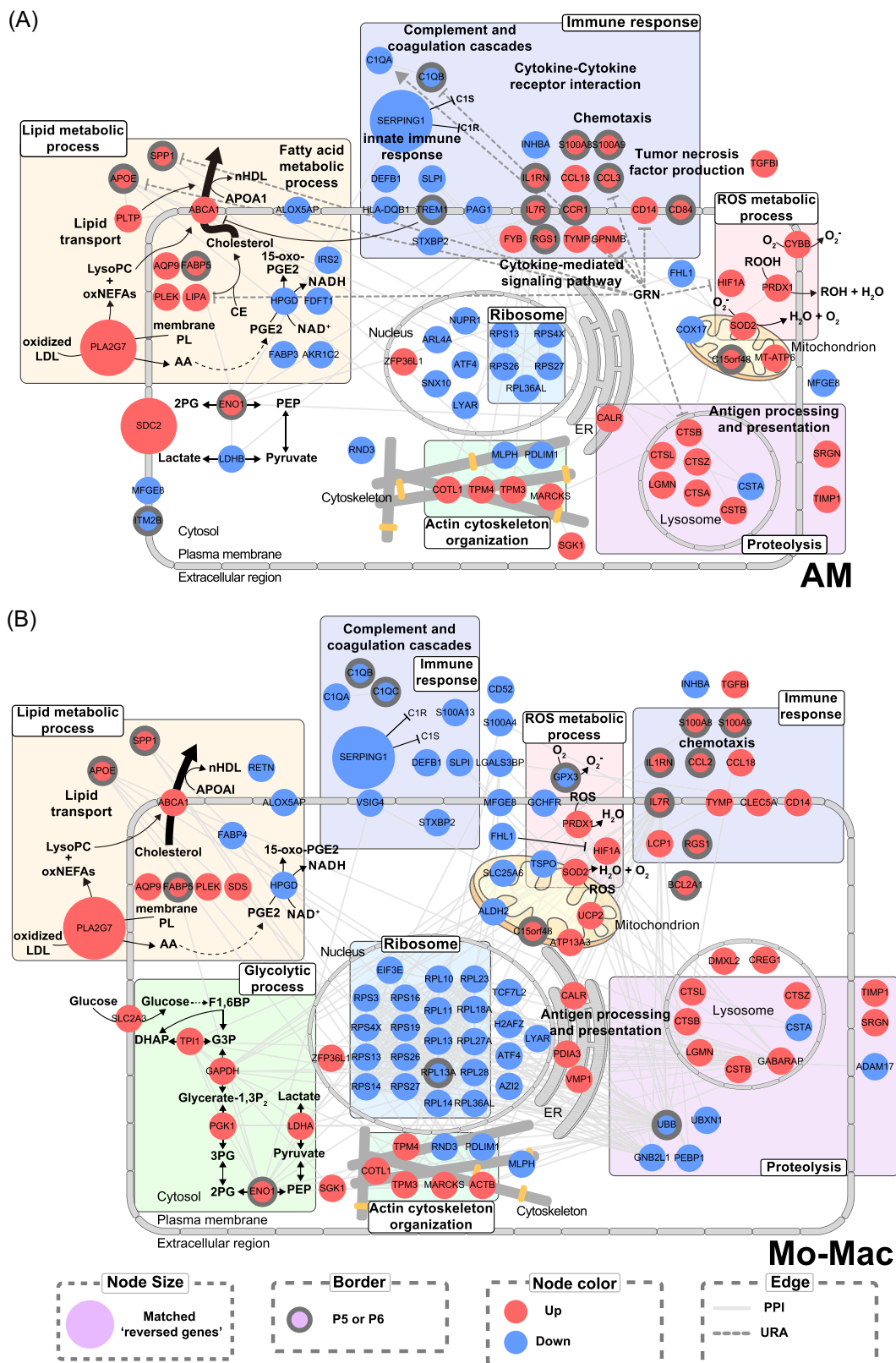
FIGURE 4 Integrated molecular network analysis in pulmonary fibrosis. (A, and B) Molecular network analysis of common differentially expressed genes (DEGs) in alveolar macrophages (A) and monocyte-derived macrophages (B) shows upregulated or downregulated common DEG expression by node color. Node size indicates whether reversed genes are matched and, by extension, whether the gene pattern for the fibrosis group or disease condition is the same. Nodes with borders are P5 or P6. The light gray edge between nodes indicates protein–protein interactions, while the dotted line extending from granulin precursor (*GRN*) shows the genes regulated by *GRN* according to the upstream regulator analysis. Genes are grouped according to their biological function determined by functional enrichment analysis. LDL, low-density lipoprotein; LysoPC, lysophosphatidylcholine; oxNEFAs, oxidized unesterified fatty acids; ROS, reactive oxygen species.

overlap of cellular mechanisms in these distinct cell types. Among the four cathepsin family genes *CTSL, CTSB, CTSZ,* and *CTSA* that are upregulated common DEGs, which code for lysosomal cathepsin proteases, *CTSL* and *CTSB* are validated in data set B-1. These two genes are recognized contributors to SARS-CoV-2 infection. However, as there is no discernible variation in their expression under the influence of the three antifibrotic drugs, pursuing them as additional targets would be potentially effective in the treatment of PCPF. Then, we performed PPI network and URA analyses to elucidate the crucial pathways implicated in PCPF treatment. *GRN* is expressed in macrophages and is the most influential element of this molecular network. It encodes progranulin, which participates in inflammation, wound healing, and lysosomal activity.[56] Increasing progranulin levels increased the proportion of regulatory T cells and reduced inflammation and apoptosis in acute lung injury models.[32] Progranulin upregulation repressed fibrotic genes and reduced liver fibrosis in animal chronic liver disease models.[57] However, other studies have reported contradictory results. Progranulin was upregulated in a mouse influenza viral infection model, and progranulin-deficient mice were protected from influenza virus-induced lung injury.[58] High serum progranulin levels were detected in COVID-19 patients.[59,60] Further research is required to clarify the role of progranulin in COVID-19 pathogenesis.

This study had certain limitations. First, data sets utilized in the comparative analysis were obtained from a limited number of sources. For IPF, only three samples were used for the single-cell analysis. Therefore, the results may not fully reflect the real heterogeneity among patients with fibrotic lung disease. While we validated our findings in the validation data set, additional research is essential to obtain more statistically supported data. Furthermore, the rat model used to study fibrosis might not fully capture the complexity of human pulmonary fibrosis. Future investigations using large sample sizes of human data are necessary to validate the foregoing findings. Second, lung transcriptomic profiles from mild COVID-19 patients without fibrosis were not available. Therefore, a direct comparison between these groups was not possible. Therefore, we are unable to provide definitive risk factors for the development of pulmonary fibrosis in COVID-19 patients. Finally, demographics and clinical biomarkers were not included in our comparative analysis. Integrating multiomics data and clinical biomarkers is necessary to identify more precise long-term COVID-19 treatment strategies. Such a comprehensive analysis would provide a deeper understanding of the disease and facilitate personalized approaches to patient care.

In conclusion, our study sheds new light on the transcriptomic changes observed in COVID-19- and IPF-related pulmonary fibrosis and the effects of antifibrotic drugs on these conditions. Moreover, our findings highlight promising therapeutic targets for PCPF. Further investigation is necessary to confirm the results presented here and to evaluate their clinical relevance for the treatment of COVID-19- and IPF-associated lung fibrosis.

AUTHOR CONTRIBUTIONS

Yumin Kim, Ji-Hwan Park, and Chang-Myung Oh designed the research. Yumin Kim, Dae-Kyum Kim, and Hyobin Julianne Lim processed and performed the computational analyses of the single-cell RNA-seq. Yumin Kim, Yeongmin Kim, and Ji-Hwan Park analyzed the bulk RNA-seq data. Yumin Kim, Ji-Hwan Park, and Chang-Myung Oh supervised the project and wrote the paper-original.

CONFLICT OF INTEREST STATEMENT

The authors declare no conflict of interest.

DATA AVAILABILITY STATEMENT

The data that support the findings of this study are available in GEO database at https://www.ncbi.nlm.nih.gov/geo/. These data were derived from the following resources available in the public domain:- GSE149878, https://www.ncbi.nlm.nih.gov/geo/query/acc.cgi?acc= GSE149878-GSE122960, https://www.ncbi.nlm.nih.gov/geo/query/ acc.cgi?acc=GSE122960-GSE158127, https://www.ncbi.nlm.nih. gov/geo/query/acc.cgi?acc=GSE158127-GSE145926, https://www. ncbi.nlm.nih.gov/geo/query/acc.cgi?acc=GSE145926-GSE120679, https://www.ncbi.nlm.nih.gov/geo/query/acc.cgi?acc=GSE120679. All transcriptome data used in our analysis have been uploaded to Gene Expression Omnibus (GEO). The single-cell RNA-seq data set A for the COVID-19 patients was deposited in GSE149878, while those for the IPF and control were deposited in GSE122960. The COVID-19 and control data used for the validation were deposited in GSE158127 and GSE145926. The bulk RNA-Seq data for the rat TGF-β1-induced pulmonary fibrosis models subjected to the three antifibrotic drugs were deposited in GSE120679. All data sets (GSE149878, GSE122960, GSE122960, GSE158127, GSE145926, and GSE120679) included in our study have been ethically reviewed and have received the necessary approvals from the original researchers in their original papers.

ORCID

Chang-Myung Oh http://orcid.org/0000-0001-6681-4478

REFERENCES

1. Wang H, Paulson KR, Pease SA, et al. Estimating excess mortality due to the COVID-19 pandemic: a systematic analysis of COVID-19-related mortality, 2020–21. *Lancet.* 2022;399:1513-1536.
2. World Health Organization. WHO Coronavirus (COVID-19) dashboard. 2023. Accessed January 19, 2023. https://covid19.who.int/
3. Lane A, Hunter K, Lee EL, et al. Clinical characteristics and symptom duration among outpatients with COVID-19. *Am J Infect Control.* 2022;50:383-389.

4. Nabavi N. Long covid: how to define it and how to manage it. *BMJ*. 2020;370:m3489.

5. Yoon HY, Uh ST. Post–Coronavirus disease 2019 pulmonary fibrosis: wait or needs intervention. *Tuberc Respir Dis*. 2022;85:320.

6. Amin BJ, Kakamad FH, Ahmed GS, et al. Post COVID-19 pulmonary fibrosis; a meta-analysis study. *Annal Med Surg*. 2022;77:103590.

7. Bazdyrev E, Rusina P, Panova M, Novikov F, Grishagin I, Nebolsin VJP. Lung fibrosis after COVID-19: treatment prospects. *Pharmaceuticals*. 2021;14:807.

8. Antony T, Acharya KV, Unnikrishnan B, Keerthi NS. A silent March-post covid fibrosis in asymptomatics–a cause for concern? *Indian J Tuberc*. 2023;70:249-252.

9. Raimundo K, Chang E, Broder MS, Alexander K, Zazzali J, Swigris JJ. Clinical and economic burden of idiopathic pulmonary fibrosis: a retrospective cohort study. *BMC Pulm Med*. 2016;16:1-8

10. Lee JY, Tikellis G, Corte TJ, et al. The supportive care needs of people living with pulmonary fibrosis and their caregivers: a systematic review. *Eur Respir Rev*. 2020;29:190125.

11. Udwadia ZF, Koul PA, Richeldi L. Post-COVID lung fibrosis: the tsunami that will follow the earthquake. *Lung India*. 2021;38:S41.

12. Mei Q, Liu Z, Zuo H, Yang Z, Qu J. Idiopathic pulmonary fibrosis: an update on pathogenesis. *Front Pharmacol*. 2022;12:797292.

13. Maher TM, Strek ME. Antifibrotic therapy for idiopathic pulmonary fibrosis: time to treat. *Respir Res*. 2019;20:1-9.

14. Finnerty JP, Ponnuswamy A, Dutta P, Abdelaziz A, Kamil H. Efficacy of antifibrotic drugs, nintedanib and pirfenidone, in treatment of progressive pulmonary fibrosis in both idiopathic pulmonary fibrosis (IPF) and non-IPF: a systematic review and meta-analysis. *BMC Pulm Med*. 2021;21:411.

15. Shchudro O, Bielosludtseva K, Pertseva T, Konopkina L, Krykhtina M, Konopkina L. Carbon monoxide diffusing capacity (DLCO) in COVID-19 survivors versus idiopathic pulmonary fibrosis (IPF): the pathogenetic features. *Eur Respir J*. 2021;58:PA3900.

16. Morse C, Tabib T, Sembrat J, et al. Proliferating SPP1/MERTK-expressing macrophages in idiopathic pulmonary fibrosis. *Eur Respir J*. 2019;54(2):1802441.

17. Xu X, Chen H, Zhu X, et al. S100A9 promotes human lung fibroblast cells activation through receptor for advanced glycation end-product-mediated extracellular-regulated kinase 1/2, mitogen-activated protein-kinase and nuclear factor-κB-dependent pathways. *Clin Exp Immunol*. 2013;173:523-535.

18. Saiphoklang N, Patanayindee P, Ruchiwit P. The effect of NINTE-DANIB in post-COVID-19 lung fibrosis: an observational study. *Crit Care Res Pract*. 2022;2022:9972846.

19. Flaherty KR, Wells AU, Cottin V, et al. Nintedanib in progressive fibrosing interstitial lung diseases. *N Engl J Med*. 2019;381:1718-1727.

20. Taniguchi H, Ebina M, Kondoh Y, et al. Pirfenidone in idiopathic pulmonary fibrosis. *Eur Respir J*. 2010;35:821-829.

21. Chen YL, Zhang X, Bai J, et al. Sorafenib ameliorates bleomycin-induced pulmonary fibrosis: potential roles in the inhibition of epithelial–mesenchymal transition and fibroblast activation. *Cell Death Dis*. 2013;4:e665.

22. Chen YL, Zhang X, Bai J, et al. Molecular characterization of a precision-cut rat liver slice model for the evaluation of antifibrotic compounds. *Cell Death Dis*. 2019;316:G15-G24.

23. Heukels P, Moor C, Von der Thüsen J, Wijsenbeek M, Kool MJRM. Inflammation and immunity in IPF pathogenesis and treatment. *Respir Med*. 2019;147:79-91.

24. Gordon EM, Yao X, Xu H, et al. Apolipoprotein E is a concentration-dependent pulmonary danger signal that activates the NLRP3 inflammasome and IL-1β secretion by bronchoalveolar fluid macrophages from asthmatic subjects. *J Allergy Clin Immunol*. 2019;144:426-441.

25. Cui H, Jiang D, Banerjee S, et al. Monocyte-derived alveolar macrophage apolipoprotein E participates in pulmonary fibrosis resolution. *JCI Insight*. 2020;5:e134539.

26. Erol A. Role of oxidized LDL-induced "trained macrophages" in the pathogenesis of COVID-19 and benefits of pioglitazone: a hypothesis. *Diabetes Metab Syndrome*. 2020;14:713-714.

27. Finkel Y, Gluck A, Nachshon A, et al. SARS-CoV-2 uses a multipronged strategy to impede host protein synthesis. *Nature*. 2021;594:240-245.

28. Tidu A, Janvier A, Schaeffer L, et al. The viral protein NSP1 acts as a ribosome gatekeeper for shutting down host translation and fostering SARS-CoV-2 translation. *RNA*. 2021;27:253-264.

29. Viola A, Munari F, Sánchez-Rodríguez R, Scolaro T, Castegna A. The metabolic signature of macrophage responses. *Front Immunol*. 2019;10:1462.

30. Li J, Zhai X, Sun X, Cao S, Yuan Q, Wang J. Metabolic reprogramming of pulmonary fibrosis. *Front Pharmacol*. 2022;13:1031890.

31. Korfei M, von der Beck D, Henneke I, et al. Comparative proteome analysis of lung tissue from patients with idiopathic pulmonary fibrosis (IPF), non-specific interstitial pneumonia (NSIP) and organ donors. *J Proteomics*. 2013;85:109-128.

32. Chen YQ, Wang CJ, Xie K, et al. Progranulin improves acute lung injury through regulating the differentiation of regulatory T cells and interleukin-10 immunomodulation to promote macrophage polarization. *Mediat Inflamm*. 2020;2020:9704327.

33. Pum A, Ennemoser M, Adage T, Kungl AJ. Cytokines and chemokines in SARS-CoV-2 infections—therapeutic strategies targeting cytokine storm. *Biomolecules*. 2021;11:91.

34. He C, Carter AB. C (C) learing the role of chemokines in pulmonary fibrosis. *Am J Respir Cell Mol Biol*. 2020;62:546-547.

35. Yang J, Agarwal M, Ling S, et al. Diverse injury pathways induce alveolar epithelial cell CCL2/12, which promotes lung fibrosis. *Am J Respir Cell Mol Biol*. 2020;62:622-632.

36. Ranjbar M, Rahimi A, Baghernejadan Z, Ghorbani A, Khorramdelazad H. Role of CCL2/CCR2 axis in the pathogenesis of COVID-19 and possible treatments: all options on the table. *Int Immunopharmacol*. 2022;113:109325.

37. Merad M, Martin JC. Pathological inflammation in patients with COVID-19: a key role for monocytes and macrophages. *Nat Rev Immunol*. 2020;20:355-362.

38. Files DC, Tacke F, O'Sullivan A, Dorr P, Ferguson WG, Powderly WG. Rationale of using the dual chemokine receptor CCR2/CCR5 inhibitor cenicriviroc for the treatment of COVID-19. *PLoS Pathog* 2022;18:e1010547.

39. Vanderheiden A, Thomas J, Soung AL, et al. CCR2 signaling restricts SARS-CoV-2 infection. *MBio*. 2021;12:e02749-21.

40. Villabona-Rueda AF, Zhong Q, Xiong Y, Palmer T, D'Alessio F. CCR2: a potential target for lung injury resolution. *Eur Respir J*. 2020;56:3350.

41. Das A, Meng W, Liu Z, et al. Molecular and immune signatures, and pathological trajectories of fatal COVID-19 lungs defined by in situ spatial single-cell transcriptome analysis. *J Med Virol*. 2023;95(8):e29009.

42. Ruiz XD, Mlakar LR, Yamaguchi Y, et al. Syndecan-2 is a novel target of insulin-like growth factor binding protein-3 and is over-expressed in fibrosis. *PLoS One*. 2012;7:e43049.

43. Wang J, Jiang M, Xiong A, et al. Integrated analysis of single-cell and bulk RNA sequencing reveals pro-fibrotic PLA2G7 high macrophages in pulmonary fibrosis. *Pharmacol Res*. 2022;182:106286.

44. Gu Y, Lawrence T, Mohamed R, Liang Y, Yahaya BH. The emerging roles of interstitial macrophages in pulmonary fibrosis: a perspective from scRNA-seq analyses. *Front Immunol*. 2022;13:923235.

45. Tall AR, Wang N. New insights into cholesterol efflux via ABCA1. *Nat Cardiovasc Res*. 2022;1:198-199.

46. Chai AB, Ammit AJ, Gelissen IC. Examining the role of ABC lipid transporters in pulmonary lipid homeostasis and inflammation. *Respir Res*. 2017;18(1):9.

47. Parimon T, Espindola M, Marchevsky A, Rampolla R, Chen P, Hogaboam CM. Potential mechanisms for lung fibrosis associated with COVID-19 infection. *QJM*. 2023;116:487-492.

48. Tomar PP, Krugliak M, Arkin IT. Blockers of the SARS-CoV-2 3a channel identified by targeted drug repurposing. *Viruses*. 2021;13:532.

49. Oshitani N, Watanabe K, Sakuma T, Matsuda M, Oyama Y. Tranilast, an antifibrotic agent and COVID-19-induced pulmonary fibrosis. *QJM*. 2022;115:249-250.

50. Soto-Heredero G, Gomez de las Heras MM, Gabandé-Rodríguez E, Oller J, Mittelbrunn M. Glycolysis–a key player in the inflammatory response. *FEBS J*. 2020;287:3350-3369.

51. Santos AF, Póvoa P, Paixão P, Mendonça A, Taborda-Barata L. Changes in glycolytic pathway in SARS-COV 2 infection and their importance in understanding the severity of COVID-19. *Front Chem*. 2021;9:685196.

52. Bhatt AN, Shenoy S, Munjal S, et al. 2-deoxy-d-glucose as an adjunct to standard of care in the medical management of COVID-19: a proof-of-concept and dose-ranging randomised phase II clinical trial. *BMC Infect Dis*. 2022;22:669.

53. Ghosh S, Dellibovi-Ragheb TA, Kerviel A, et al. β-Coronaviruses use Lysosomes for egress instead of the biosynthetic secretory pathway. *Cell*. 2020;183(6):1520-1535. doi:10.1016/j.cell.2020.10.039

54. Meyer B, Chiaravalli J, Gellenoncourt S, et al. Characterising proteolysis during SARS-CoV-2 infection identifies viral cleavage sites and cellular targets with therapeutic potential. *Nat Commun*. 2021;12(1). doi:10.1038/s41467-021-25796-w

55. Yuan L, Zou C, Ge W, et al. A novel cathepsin L inhibitor prevents the progression of idiopathic pulmonary fibrosis. *Bioorg Chem*. 2020;94:103417.

56. Lan YJ, Sam NB, Cheng MH, Pan HF, Gao J. Progranulin as a potential therapeutic target in immune-mediated diseases. *J Inflamm Res*. 2021;14:6543.

57. Yoo W, Lee J, Noh KH, et al. Progranulin attenuates liver fibrosis by downregulating the inflammatory response. *Cell Death Dis*. 2019;10:758.

58. Luo Q, Yan X, Tu H, Yin Y, Cao J. Progranulin aggravates pulmonary immunopathology during influenza virus infection. *Thorax*. 2019;74:305-308.

59. Özgeriş FB, Koçak ÖF, Kurt N, Parlak E, Yüce N, Keleş MS. High serum progranulin levels in COVID-19 patients: a pilot study. *Biochemistry (Mosc)*. 2022;87:207-214.

60. Rieder M, Wirth L, Pollmeier L, et al. Serum protein profiling reveals a specific upregulation of the immunomodulatory protein progranulin in coronavirus disease 2019. *J Infect Dis*. 2021;223:775-784.

SUPPORTING INFORMATION

Additional supporting information can be found online in the Supporting Information section at the end of this article.